JTTEE5 19:1115–1130
DOI: 10.1007/s11666-010-9511-2
1059-9630/$19.00 © ASM International

Study of the Splat Microstructure, Splat-Substrate Interface, and the Effects of Substrate Heating on the Splat Formation for Ni-Cr Particles Plasma Sprayed on to Aluminum Substrates

S. Brossard, P.R. Munroe, A.T.T. Tran, and M.M. Hyland

(Submitted February 17, 2010; in revised form April 16, 2010)

This study investigates the mechanisms of formation of plasma-sprayed coatings, through the study of splat morphology and the splat-substrate interface of NiCr single splats sprayed onto Al substrates, at both micro- and nano-scale levels, using a range of electron microscopy techniques. This study provides direct observation of extensive substrate melting, together with chemical inter-mixing with the splat and the formation of metastable interfacial phases (including both non-equilibrium phases and metallic glasses). In addition, voids and a range of oxide phases were observed. The mechanisms of formation of these features are discussed. Two aluminum alloys (with and without Mg additions) and three different sets of substrate surface conditions (polished, and heat treated prior to and during spraying) were used to investigate the variations in splat morphologies induced by the different preparation conditions. It was found that the heating of substrate during spraying significantly reduced splashing.

Keywords aluminum, interface, nickel chromium, oxide, plasma spray, splat

1. Introduction

In the past few decades, a number of methods have been developed to modify the surface characteristics of materials. These methods include thermal spray processing, which is based on the projection of particles, most usually melted onto a substrate, to build a surface coating. In the case of plasma spraying, a plasma flame is used to melt the sprayed particles. Its large range of temperatures (500-25,000 °C), along with the variability in the particle velocity (80-300 m s^{-1}), material (any with a congruent melting point), and size distribution (from 5 to 50 μm for ceramics, 20-120 μm for metals), gives to the process significant flexibility and versatility (Ref 1-3).

The study of the formation of the plasma-sprayed coatings is critical for improving their performance. Indeed, properties, such as thermal and electrical conductivity, density, wear resistance, or adhesion strength, may be significantly influenced by factors such as the oxide content (which can form in-flight or during the coating formation), void content (usually ~1 to 5 vol.%), or the bonding between the coating and the substrate (Ref 1, 2). Furthermore, coatings are built up by the accumulation of the sprayed particles which flatten on impact, forming ''splats.'' Consequently, studying coating formation implies studying splat formation, especially, of the splats which impact directly on to the substrate.

Therefore, the formation of single splat has often been studied through the observation of their morphology (Ref 4, 5) or the characteristics of the substrate (especially surface chemistry and topography; Ref 6-11). Notably, it was found that splashing of splats on impact with the substrate and spreading was an important phenomenon that was significantly reduced by heating the substrate above a certain temperature (called transition temperature) during the spray process (Ref 5, 6, 12-15). This, in turn, may be associated with the desorption of asdorbates/condensates present on the substrate surface (Ref 6, 12, 13, 16), or by the splat solidification starting before flattening was complete (Ref 5, 15, 17, 18) (both phenomena may, however, be avoided by the heating of the substrate during spraying). Adhesion of the coatings was also found to increase when heating the substrate during spraying (Ref 19). The mechanisms of splat formation have also been studied using in situ experiments with millimeter-sized droplets (Ref 8, 20-23) or by modeling (Ref 21, 24, 25).

However, studies on the direct interaction between splat and substrate and of the splat microstructure at a high resolution are very limited due to the difficulty in

S. Brossard and **P.R. Munroe**, School of Materials, University of New South Wales, Sydney, NSW 2052, Australia; and **A.T.T. Tran** and **M.M. Hyland**, Chemical & Materials Engineering Department, University of Auckland, Auckland 1142, New Zealand. Contact e-mail: sophie.brossard@student.unsw.edu.au.

preparing specimens from local and precise regions of the splat-substrate interface. Kitahara and Hasui (Ref 26) studied the coating-substrate interface for various sprayed material/substrate combinations, including Ni particles sprayed onto an Al substrate, and found in that case, using x-ray diffraction, that an intermetallic phase, identified as Al_3Ni, was present at the interface. This was then interpreted as evidence of local substrate melting. The occurrence of local substrate melting and formation of an intermetallic phase was also found in a small number of other cases involving substrates other than Al; for example, Mo sprayed on steel, with the formation of Fe_2Mo, which was observed by transmission electron microscopy (TEM) (Ref 5, 27). However, in a prior study by the authors, no evidence of substrate melting or mixing between splat and substrate materials was observed for plasma-spray of NiCr on aluminum (Ref 28). However, the spray conditions in that study were different to those used by Kitahara and Hasui (Ref 26). The occurrence of substrate melting and intermixing between splat and substrate are of critical importance as they show the incidence of metallurgical, rather than mechanical, bonding, which may lead to improved adhesion of the coating.

Consequently, the aim of this study is to observe the microstructural features of single splats, with a particular emphasis on the splat-substrate interface. The sprayed material was NiCr, which is commonly used in plasma spray coatings for applications such as wear resistant coatings or bond coats, including on aluminum substrates. Substrates were made of two aluminum alloys (5052 and 1005, alloys differing most notably by their Mg content) and submitted to various treatments: polished, thermally treated prior to spraying or heated during spraying, modifying the surface chemistry to study how this may affect splat characteristics and formation. Indeed, surface chemistry and topography, as induced by heat treatments, has been shown to have a significant influence on splat morphology. Cedelle et al. (Ref 8) for example found that heat treating stainless steel, by inducing, amongst other things, a positive skewness, increased the wetting of the sprayed molten NiCr particles, giving thinner splats. Moreover, a previous study by the authors found that such treatments reduced the occurrence of substrate melting (Ref 29). Studies with aluminum substrates have also shown that boiling in distilled water created a thick boehmite layer γ-AlOOH preventing adhesion of the splats (Ref 28). Moreover, as mentioned earlier, heating during spraying above the transition temperature was found to produce very disc-shaped splats instead of irregularly shaped ''splashy'' splats.

As a result, the splat morphology and microstructure have been then investigated using a range of electron microscopy techniques, resulting in unambiguous evidence of substrate melting the formation of non-equilibrium phases resulting from rapid solidification and intermixing of the splat and substrate. The observations made were then used to discuss the splat formation process and the effect of heat treatment of the substrate.

2. Experimental Procedure

Five different substrates were used, prepared from two aluminum alloys 5052 and 1005. Al 5052 contains Mg (2.2-2.8 wt.%), which is expected to become oxidized to form a very thin layer of MgO on top of the substrate surface and modify the surface chemistry (Ref 28, 30), while Al 1005 contains very limited amounts of Mg ($\leq$0.05%). The different substrates and their pre-treatments are listed in Table 1.

All substrates were first mechanically ground and mirror polished with diamond paste, to a nanoscale roughness (~7 nm). The thermally treated substrates (Al1005_PT and Al5052_PT) were heated at 350 °C for 90 min in air, but spraying was performed at room temperature several hours after the specimens had cooled, meaning that for instance moisture from the air may have readsorbed on the substrates' surface. The substrate heated during spraying (Al5052_PH) was heated at a temperature of 350 °C 30 min before spraying and held at the same temperature during spraying. The aim of these thermal treatments is to form surface oxides, and/or to induce some level of surface roughness. Furthermore, the water chemisorbed on the substrate surface is expected to be released from the substrate at this temperature (Ref 31).

The sprayed material was a commercial NiCr alloy powder (Ni80-Cr20, Sulzer Metco 43 VF-NS, Switzerland, $(-45+5)$ μm). Plasma spraying was carried out with a Sulzer Metco (Switzerland) 7 MB gun (with a nozzle diameter of 8 mm), operating at a current of 550 A and at a voltage of 62 V, with a spraying distance of 100 mm. The feeding rate of the powder was of 1 g/min, the carrier gas being argon at a flow rate of 3 SLPM, while the plasma gas was a mixture of nitrogen and hydrogen, at a flow rate of 47.5 and 6.2 SLPM, respectively.

The specimens were then characterized using a range of analytical techniques. A Hitachi S3400 scanning electron microscope (SEM) was used to image the overall morphology of the splats and the substrates. A FEI xP200 Focused Ion Beam microscope (FIB) was used to mill cross sections of the splats using an energetic gallium ion beam, and to image them using secondary electrons induced by the ion beam. Details have been described elsewhere (Ref 32). A FEI xT Nova Nanolab 200 dual beam microscope (that is a FIB and SEM combined into a single instrument) was used to prepare cross sections of splats (100-200 nm in thickness) suitable for TEM observation. These were prepared using the lift-out method as

Table 1 Substrate nomenclature and condition

Specimen	Substrate	Pre-treatment
Al5052_P	Aluminum 5052	Polished (to nanoscale smoothness)
Al5052_PT	Aluminum 5052	Polished and thermally treated
Al5052_PH	Aluminum 5052	Polished and heated during spraying
Al1005_P	Aluminum 1005	Polished (to nanoscale smoothness)
Al1005_PT	Aluminum 1005	Polished and thermally treated

described elsewhere (Ref 32) and examined in a Philips CM200 transmission electron microscope (TEM) to which energy dispersive x-ray spectroscopy (EDS) facilities have been interfaced. Finally, the average surface roughness of the polished substrates was measured using a Digital Instruments DI3000 Atomic Force Microscope (AFM).

Several FIB and TEM cross sections were prepared and studied for each particular feature and/or type of splat. However, for reasons of brevity, only a small number of representative images will be presented here. The cross section preparation process using FIB also involves the deposition of a layer of platinum on top of it prior to milling for protection purposes. This layer is present on the FIB and TEM images presented.

3. Results and Discussion

The splats, and their formation, are described from electron microscopy observations.

Because of their overall similarity, the splats on the polished and polished and thermally treated substrates are detailed in a first part, then, in the second part, splats formed on the substrate heated during spraying are described and discussed. Details on the roughness of the substrates surface can be found in a previous publication (Ref 28).

3.1 Description of the Splats Found on the Polished and Polished and Thermally Treated Specimens

3.1.1 Various Splats Morphologies Found on the Different Specimens. SEM images of 50-60 splats were taken for each specimen. Figure 1 displays some SEM images of typical splats. Different types of morphology were observed and are described below:

- Many of the splats displayed a very characteristic morphology, with a ring of splashed fingers around the central core of the splat (marked 1 on Fig. 1a). They will be denoted as ''RSF splats''.
- Some have an almost circular shape, with no, or limited, splashed fingers (Fig. 1b). They will be called ''circular splats''.
- Other splats have no, or limited, splashed fingers, but a very irregular shape (Fig. 1c). They will be called ''irregularly shaped splats''.
- On both polished substrates (Al5052_P and Al1005_P), a very small number of splats were also found which displayed a ring of splashed fingers, but the central core of the splat was also very fragmented (Fig. 1d).

The diameter D was evaluated for each splat by measuring the smallest and largest values and taking the average, ignoring the splashed fingers. However, for

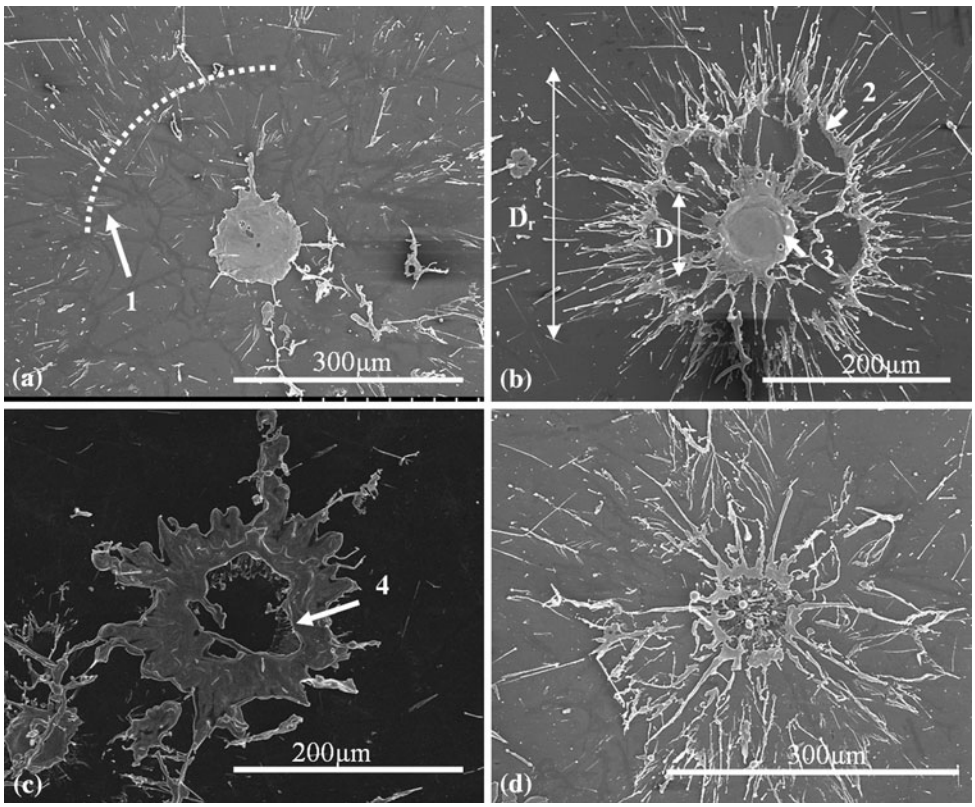

Fig. 1 SEM images of the different types of splats found on all of the substrates sprayed at room temperature: (a) halo splat, (b) halo fingered splat, (c) halo doughnut splat, and (d) fragmented splat

splats with a ring of splashed fingers, the diameter D_r for this ring was also measured and expressed as a function of the diameter of the splat itself (see Fig. 1a for example). The average diameter and the relative proportion, P, for each category of splats for each specimen are presented in Table 2. The few splats found with a ring of splashed fingers and a fragmented center were not taken into account due to their very low frequency of observation. Examining of the values displayed in Table 2, and considering the errors resulting from the fact that the values presented were calculated for only a relatively limited amount of splats, it can be noted that the different types of splats are present in very similar proportions on all the four substrates. However, some variations may be observed in the average diameters of the splats between the non-heat treated and the heat-treated specimens.

Table 2 Relative proportions and average diameter of the splats (and average diameter of the ring of splashed fingers if applicable) found on polished and polished and thermally treated Al substrates

	Al5052_P	Al1005_P	Al5052_PT	Al1005_PT
RSF splats				
P	55%	56%	60%	51%
D_m	[92 ± 30] μm	[89 ± 26] μm	[110 ± 47] μm	[115 ± 51] μm
D_r	[2.7 ± 1.0] D	[3.4 ± 1.7] D	[2.6 ± 0.9] D	[1.9 ± 0.8] D
Circular splats				
P	16%	19%	17%	26%
D_m	[58 ± 36] μm	[78 ± 32] μm	[28 ± 6] μm	[23 ± 8] μm
Irregularly shaped splats				
P	29%	25%	23%	23%
D_m	[100 ± 46] μm	[119 ± 40] μm	[138 ± 44] μm	[136 ± 35] μm

3.1.2 Microstructure and Formation Process of the RSF Splats. Figure 2 displays three FIB cross sections made across a RSF splat. The inset image shows the location of each cross section on the splat. It can be observed that all along the central part of the splat (see the zones marked 1 on Fig. 2a, b), contact between the splat and the substrate is very good. Toward the periphery of the splat, jetting of the Al substrate within the splat, and mixing of both splat and substrate can be seen (for example, marked 2 on Fig. 2b). This shows that substrate melting has occurred. When examining the splat-substrate interface by TEM, such as the cross section presented in Fig. 3, the interface appears irregularly shaped and indistinct (1), as seen on the bright field image (Fig. 3a) and on the elemental EDS maps (Fig. 3b, c). However, a very specific structure can be observed at the interface. On the bright field image (Fig. 3a), a layer exhibiting a darker contrast than the Al substrate can be seen just under the splat interface (1), which is also very irregularly shaped. On the higher magnification bright field image (Fig. 3e), it can be seen that there are actually two layers. The layer adjacent to the NiCr splat appears amorphous (2), as no grain structure can be observed. Moreover the electron diffraction pattern obtained for this area only displayed a very diffuse ring, consistent with being a glassy phase. The second layer appears to be composed of very fine grains, firstly equiaxed (3), then, closer to the Al substrate, more needle-like grains can be observed (4). The electron diffraction pattern obtained from the finely grained layers

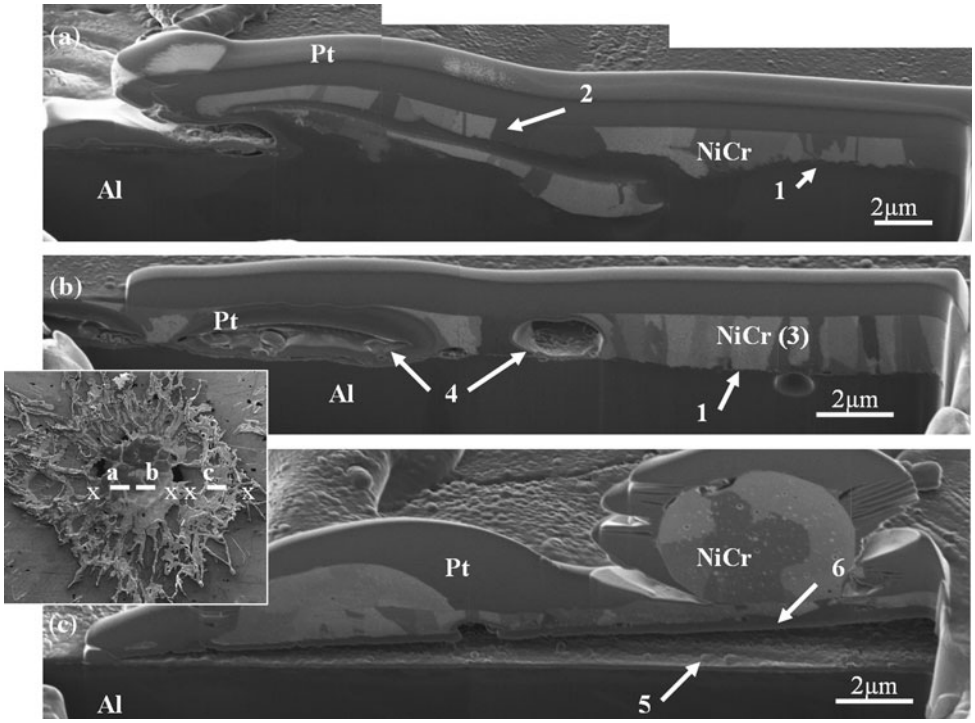

Fig. 2 FIB cross sections of a RSF splat (see inset picture) found on Al1005_P

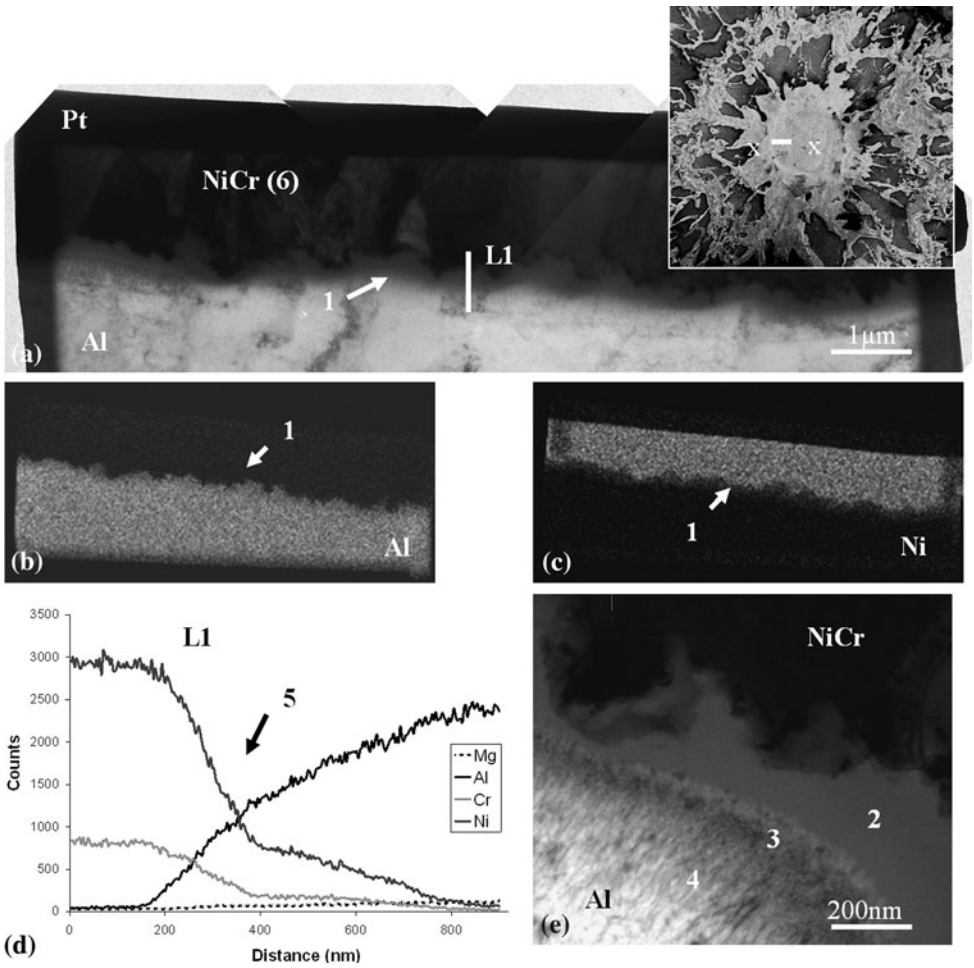

Fig. 3 TEM cross section made across a RSF splat (see inset picture) found on Al5052_P: (a) bright field image, EDS elemental maps for (b) Al, (c) Ni, (d) EDS elemental linescan, (e) high magnification bright field image of the splat-substrate interface

exhibits an irregular array of reflections. Thus, it was not possible to obtain an unambiguous identification of an interfacial phase. However, on the elemental linescan, L1, performed across the interface (Fig. 3d), one can note that the variations in the Al and Ni concentrations are not sharp, but gradual (5), showing interdiffusion has occurred over a distance of more than 500 nm (which is large compared to the electron probe size that is estimated to be ~5 nm in diameter). Moreover, there is no step-like change in composition, but an almost uniform change, thus ruling out the presence of a stochiometrically defined intermetallic phase. The most possible explanation would be these are metastable phases, with a layer of metallic glass and a layer made of non-equilibrium Ni-Al crystalline phases. Hung et al., when studying glass formation in the Al/Ni system, found that intermetallic compounds, such as Ni_3Al and $NiAl_3$, were able to be amorphized, while NiAl would remain crystalline (Ref 33). The presence of these glassy and metastable phases shows that solidification must have occurred at a very high rate, and as shown by the columnar shape of the grains composing the splat (see 3 on Fig. 2a and 6 on Fig. 3a), the heat is removed mainly through the substrate.

The interfacial layers described are not uniform. As it can be seen on the TEM cross section presented in Fig. 4, the splat-substrate interface may, in some areas, be straight and defined (1), with no evidence of substrate/splat mixing, juxtaposed to zones of substrate melting (2). The linescan, L1, performed across the interface in such zone show sharp variations in the concentration of Ni and Al (see 3 on Fig. 4f), in comparison with the linescan L2 (see 4 on Fig. 4g) acquired across the zone of substrate melting, denoting the absence of melting. On the EDS elemental maps (Fig. 4d, e), segregation of Cr in a thin layer may also be observed (5), which most likely occurred by the oxidation of Cr leading to the formation of an oxide, most probably Cr_2O_3. Such oxidation process may have occurred in-flight (Ref 12) or upon splat solidification and cooling down from the gases released either from the substrate or from the splat (Ref 34) (the gas release process is discussed in more detail later).

In the center of the splat, some large voids (up to 10 μm in diameter) were often noted to be present. These may be located either within the splat, such as on Fig. 2(b) (4) and Fig. 4(a) (6), or within the substrate, for example those present in the TEM cross section presented Fig. 5.

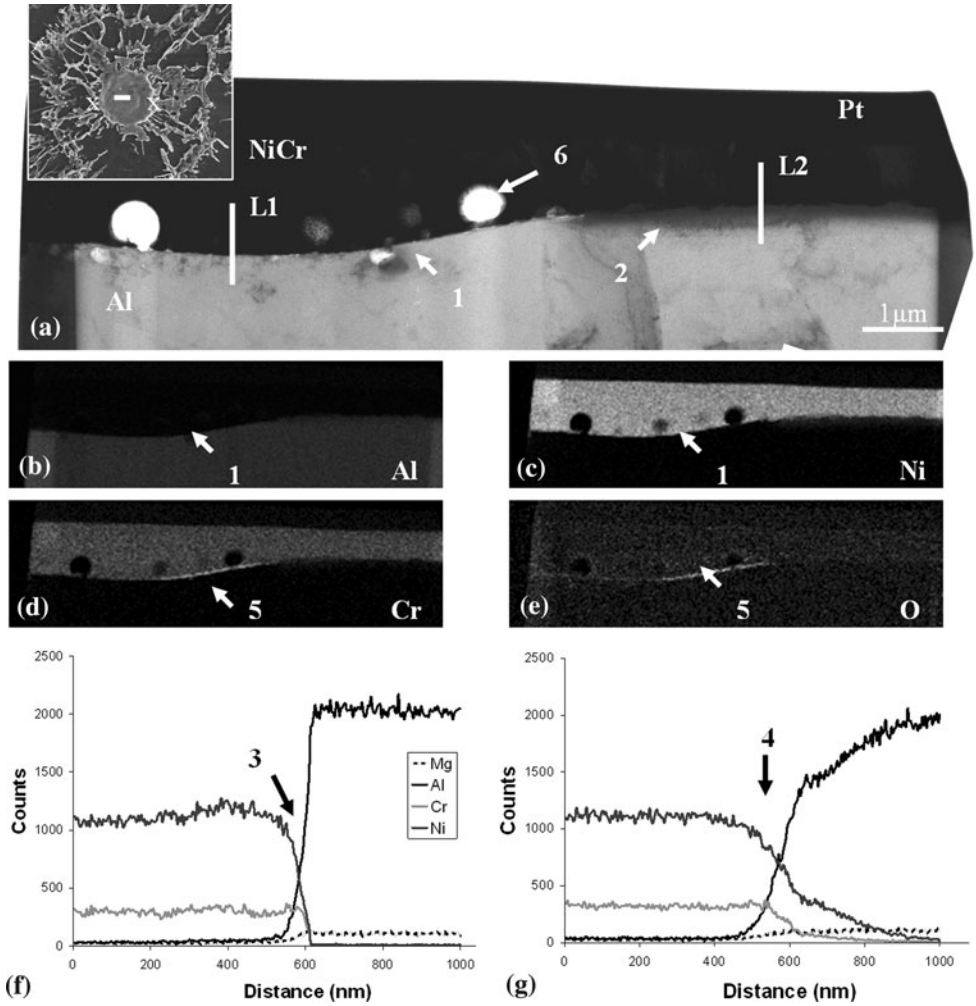

Fig. 4 TEM cross section made across a RSF splat (see inset picture) found on Al1005_P: (a) bright field image, EDS elemental maps for (b) Al, (c) Ni, (d) Cr, (e) O, (f and g) EDS elemental linescans

Dense and thick oxide layers are often found on the walls of such voids. EDS elemental maps (Fig. 5b, e) and electron diffraction studies (see diffraction pattern presented Fig. 5f) suggest that this layer may be alumina γ-Al_2O_3 (1). On the bottom surface of the void, however, the EDS elemental maps (Fig. 5c-e) show that the layers of oxide contains not only Al, but also Ni and Cr (2), it therefore may be a mix of spinel $NiAl_2O_4$, as identified by the electron diffraction pattern presented Fig. 5(g) (despite being made of poorly defined rings) and Cr_2O_3, or the spinel $NiCr_2O_4$, which has a similar diffraction pattern to $NiAl_2O_4$. All these oxides species are expected to form on alloys containing Al, Ni and Cr (Ref 35).

Figure 2(c) shows a FIB cross section prepared across a splashed finger at the periphery of the splat: it appears that here the contact between splat and substrate is very poor (5). The poor adhesion between these phases was possibly associated with the accommodation of stresses arising during the cooling of the splat, such that the splat gets lifted-up above the substrate. This phenomenon has often been observed before (Ref 36), and has been denoted as curling-up. An oxide, identified as Al_2O_3, was found to have form on the bottom surface of the splat in these locations (6). Some Al may have adhered to the bottom surface on the splat when it was still in contact with the substrate, and upon lifting-up, have become oxidized to form alumina.

Previous studies attributed, at least partly, the occurrence of splashing to desorption of adsorbates/condensates present on the substrate surface, causing the formation of an instable gas cushion (Ref 6, 12, 13, 16). Qu and Gouldstone also suggested the release of gas from the splat itself during solidification and cooling, in which gas would have been dissolved upon impact due to the pressure build-up (Ref 34). The presence of oxides in voids observed here, or on the bottom surface of the splat where curling-up has occurred, may be seen as an evidence of such gas release, as it shows that hot oxidizing gases were present, either entrapped in the voids formed, or pushed toward the periphery of the splat by the flowing molten NiCr. However, while the small voids (<4 μm) present within the substrate as shown in Fig. 2(b) (4) have most

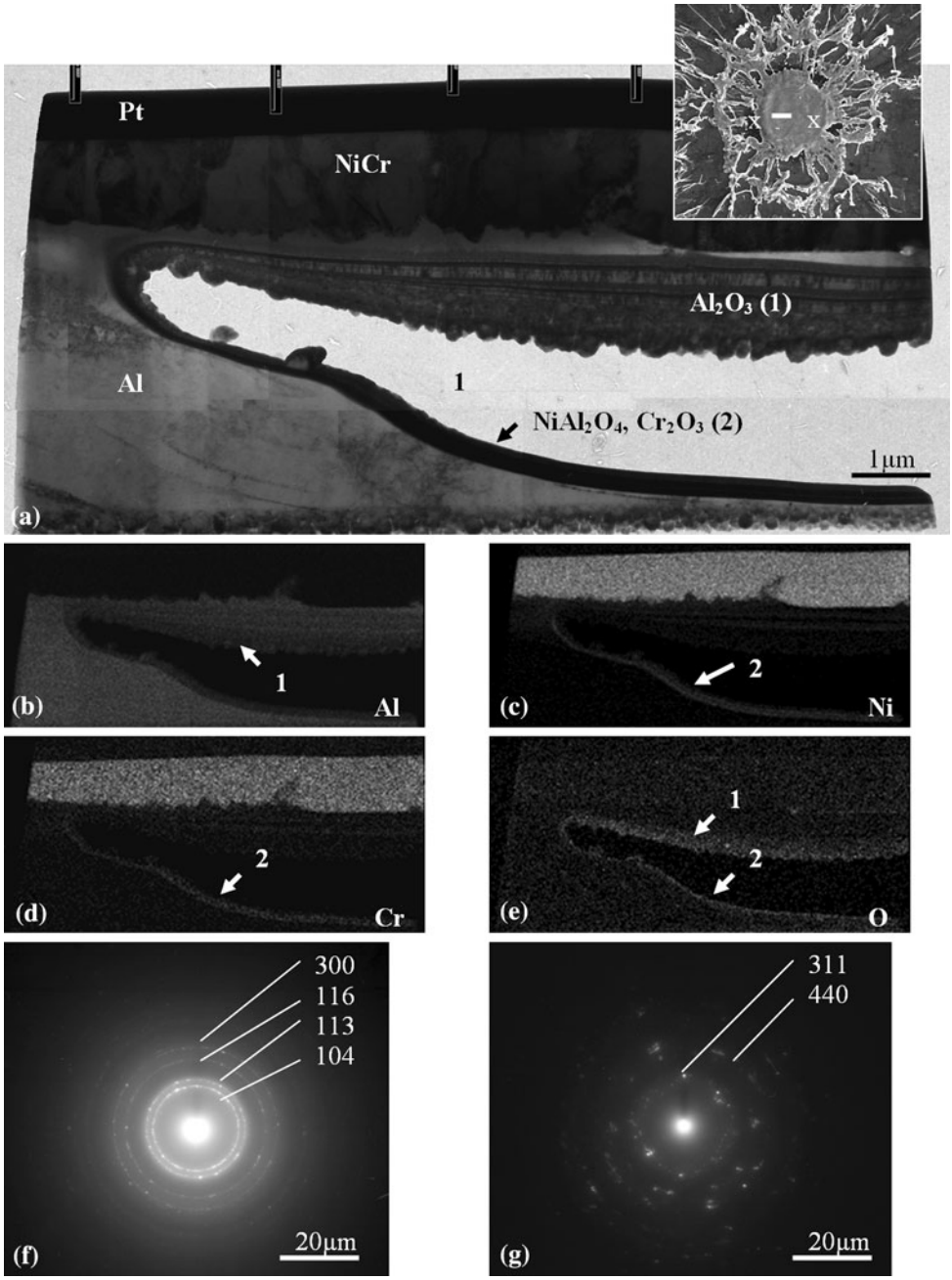

Fig. 5 TEM cross section made across a RSF splat (see inset picture) found on Al5052_PT: (a) bright field image, EDS elemental maps for (b) Al, (c) Ni, (d) Cr, (e) O, electron diffraction pattern for (f) γ-Al_2O_3, (g) spinel $NiAl_2O_4$

probably formed from gas bubbles (Ref 34), it should be noted that the size and location of the very large voids seen within the substrate, see Fig. 5, indicate that they may have been formed by a different process. Modeling of the splat formation process, which usually does not take substrate melting into account, has shown that central voids are often formed because of the mechanics of the flow of the spreading splat, due to the change in curvature of the droplet upon impact (Ref 23, 37). The mixing between Al and NiCr observed toward the periphery of the splat, such as seen Fig. 2(a) (2), suggests turbulence of the flow of such molten materials. Some voids may also be formed in this region, similar to the ones found toward the center of the splat within the substrate. Mixing of the two phases also contributes to the splat, displaying a raised ring close to the rim, which can be seen in the SEM images (see for instance the region marked 2 on Fig. 1a). The presence of such a ring may then allow prediction of those splats, which have undergone substrate melting, solely from inspection of a SEM image.

3.1.3 Microstructure and Formation Process of the Other Types of Splats. Figure 6 shows the FIB cross section of a splat with a ring of splashed fingers, but with a highly fragmented central portion. One can note the very poor contact between the splat and substrate (1), along with the thin, but dense layer present on the bottom surface on the splat (2), which was identified using TEM as being α-Al_2O_3, formed, most possibly, by the same process as described previously for the RSF splats. The splat is also very thin (<1 μm), and the grains are, in comparison, quite coarse (~2 μm) (3), which suggests a relatively slow solidification linked to the poor contact between splat and substrate and, consequently, the high thermal contact resistance hindering the heat removal through the splat-substrate interface. The very poor adhesion, linked to the poor contact, may explain why relatively few of these splats were observed, as they may be prone to delaminate from the substrate. Finally, the presence of the splashed fingers and oxide layers, along with the absence of substrate melting, shows that splashing of the splat probably arises from gas release from the substrate, rather than instabilities due to melting of the substrate.

Figure 7 shows a FIB cross section across a circular splat. The splat-substrate interface appears straight and distinct (1), while the contact between splat and substrate is mostly good. The splat grain structure is fine and columnar (<1 μm) (2), indicating a relatively fast rate of solidification with the heat removed mainly through the substrate, which is presumably linked to the good contact observed. Some fine voids were observed at the interface (3), probably formed from the gas released from the substrate. The rim of the splat has also been slightly lifted-up (4) due to the curling up process.

The various oxides phases present on such splats were identified using TEM, as shown in Fig. 8. In voids (1), like the RSF splats, alumina γ-Al_2O_3 was found (2), identified by both EDS elemental maps (see Fig. 8b, e) and electron diffraction. A dense thin layer of Cr_2O_3 was also observed on the outer surface of the splat (3), as seen on both Cr and O elemental maps (Fig. 8d, e). It was identified by electron diffraction as being Cr_2O_3 (see Fig. 8f, which could be identified as Cr_2O_3). Spinel $NiCr_2O_4$ was also found to form at the base of one of the voids (4). Such phases were found to form often on sprayed NiCr splats in previous studies (Ref 38, 39). Cr_2O_3 layers were also observed locally at the splat-substrate interface (5). While the formation process of Cr oxide on the outer surface of the splat is well understood and has been explained before (Ref 40), the manner in which the oxide may found at the interface is not clear. Indeed, it cannot have formed from the oxidation of the substrate, and thus it must have arisen from the oxidation of the NiCr particle. Fukumoto et al. previously reported Cr oxide (CrO_3 and Cr_2O_3) formed on the NiCr particle in-flight (Ref 12). Consequently, this may be the origin for the oxide observed here; however it is surprising that it is present in such a flat film shape.

It can be noted that for all these splats, neither substrate melting, nor mixing with the NiCr splat, was observed. Moreover, as it can be seen on the SEM images (see Fig. 1b, c), the outer surface of the splat is smooth; the raised ring pattern observed previously for the RSF splats, due to the substrate melting, is absent.

3.1.4 Summary of the Splat Formation Process. When the NiCr particles impact on the substrate, they are, mostly, in a fully molten state—thus at a temperature at least equal to the melting point of NiCr (~1400 °C), which

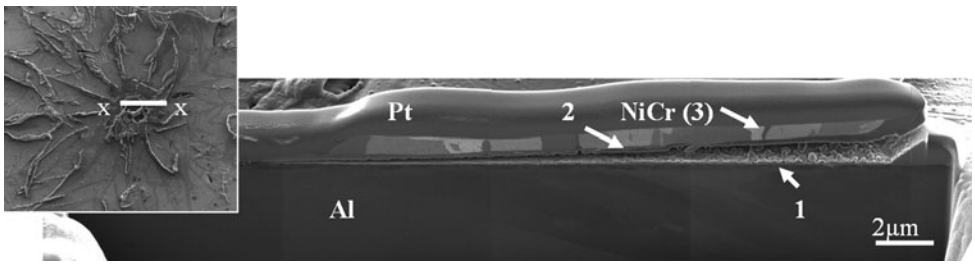

Fig. 6 FIB cross section of a very fragmented splat with a ring of splashed fingers (see inset picture) found on Al5052_P

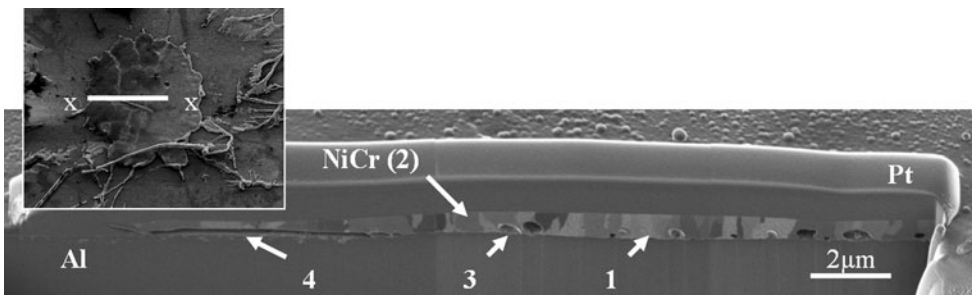

Fig. 7 FIB cross section of a circular splat (see inset picture) found on Al1005_P

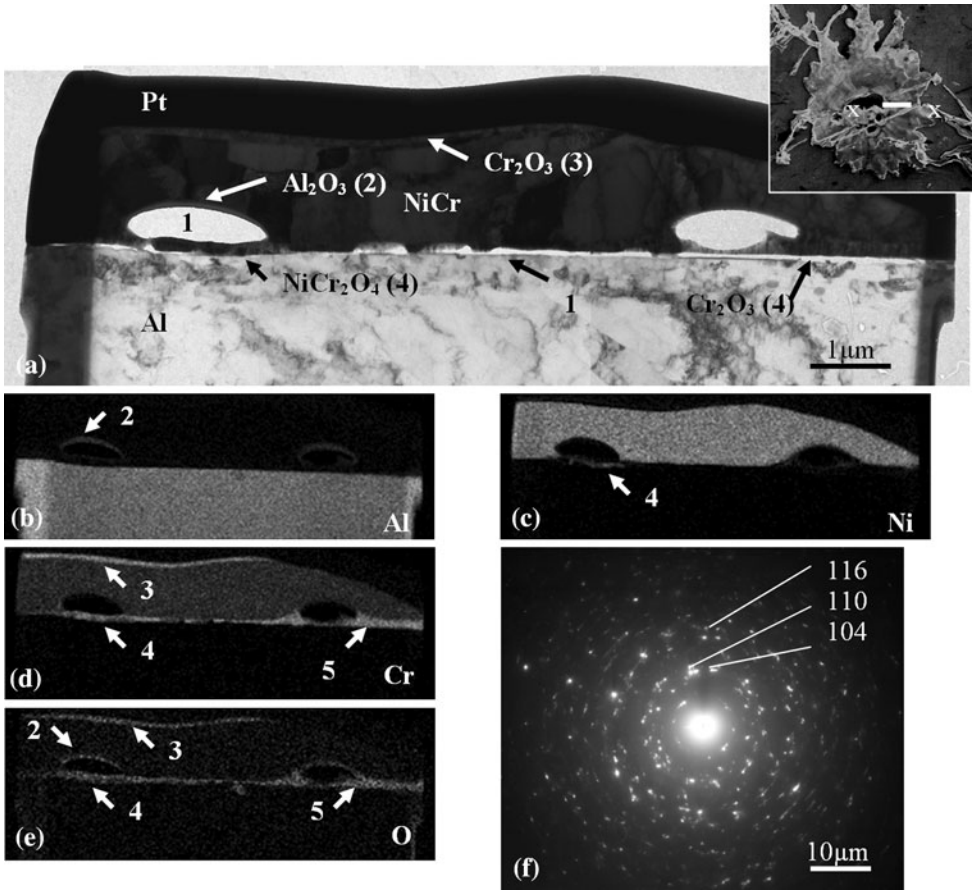

Fig. 8 TEM cross section made across a RSF splat (see inset picture) found on Al5052_P: (a) bright field image, EDS elemental maps for (b) Al, (c) Ni, (d) Cr, (e) O, (f) electron diffraction pattern for Cr_2O_3

is significantly higher than the melting point of aluminum (649 °C). Consequently, localized melting of the substrate may be expected, and this was clearly observed for the RSF splats. The depth of the substrate melting is up to several microns, as indicated by the depth of voids or zones of NiCr-Al mixing. It should also be noted that the occurrence of substrate melting was accompanied by the presence of a dense ring of splashed fingers. For the circular and the irregularly shaped splats, there was no, or very limited, splashed fingers. In a previous study, where NiCr particles were also plasma sprayed onto aluminum substrate, but where no substrate melting was observed, the splats also exhibited no, or limited, splashed fingers (Ref 28). While previous studies attributed desorption of asdorbates/condensates, such as chemisorbed water, from the substrate for the occurrence of splashing (Ref 6, 12, 13, 16), the observations made here lead to the hypothesis that the formation of such characteristic ring of splashed fingers may also be linked to the instability encountered by the spreading NiCr particle on the molten substrate. Some studies have also related the start of solidification of the splat before the end of the spreading process as a cause of the splashing (Ref 5, 15, 17, 18). In such cases, the good contact between splat and substrate for the RSF splats would promote splat solidification, which would be more likely to be inhibited for the irregularly shaped splats where the contact is poorer. Finally, for the few irregularly shaped splats with a ring of splashed fingers, they may be cause by the release of a significant amount of gas from the substrate, creating a gas cushion hindering, on one hand, the contact with the substrate and, thus, the degree of substrate melting, and, on the other hand, such instability causing the extended splashing.

As a result, the formation process may be summarized as follows: upon impact of the molten NiCr particle, ''impact splashing'' was reported to occur (Ref 20, 41), causing the rebound of small molten NiCr droplets which, when falling back onto the substrate, with a momentum and temperature that are insufficient to create substrate melting, but the droplets would then form small circular splats, which may undergo significant oxidation due to the vicinity of hot gases from the flame for example, causing the formation of oxides such as Cr_2O_3.

On the other hand, in the case of the RSF splats, upon impact and spreading of the NiCr particle, heat is transmitted to the Al substrate, causing desorption of asdorbates/condensates present on the substrate, and localized substrate melting. Both phenomena, along perhaps with the starting of the solidification of the splat, may result in disturbing the flow of the spreading molten particle,

translating in the mixing of Al and NiCr toward the splat periphery, as the molten substrate gets carried and jetted by the flowing NiCr, resulting in the formation of a ring of splashed fingers. Owing to the mechanics of the flowing splat forming, as described by some previous modeling studies (Ref 23, 37), large voids may form within the substrate either toward the center of the splat or toward the periphery, when mixing between NiCr and Al takes place. The presence of gas at the interface of the substrate and the forming splat also plays a role, leading to potential smaller voids at the splat-substrate interface. Furthermore in many cases, toward the center of the splat, this may lead to the formation of oxides such as Al_2O_3 or $NiCr_2O_4$. The formation of such bubbles was studied by Qu et al., who suggested that such gases may come from desorption of species adsorbed on the substrate surface, but also gas which becomes dissolved within the molten sprayed droplet upon impact, and released upon cooling down (Ref 34).

When the molten Al and NiCr solidify, they solidify to a very fine grain structure or a metallic glass. This suggests that solidification must occur very quickly. Moreover, such phases are evidence of metallurgical bonding between splat and substrate in this zone. This may be seen as beneficial for the adhesion strength of the coating, provided that the interfacial layers are not brittle. It has been observed that compared to crystalline metals, metallic glasses are significantly more brittle (fracture may occur at stress levels around 100 times less than the ones observed for the corresponding crystalline metal) (Ref 42). This, however, is not sufficient to determine the actual influence of the metallic glass layer on the adhesion properties of the coating.

These observations are with respect to the main, central, part of the splat; indeed, toward the splat periphery, notably for the splashed fingers, the contact between substrate and splat is poor and no substrate melting takes place.

Upon splat solidification and cooling down, curling up of the splat occurs, to accommodate the rise of thermal stresses, and the peripheral parts of the splat that have not strongly adhered to the substrate. This occurs at the rim of the splat or splashed fingers linked to the central part of the splat, get lifted-up. Some Al attached to the bottom surface of the splat in these zones then gets oxidized, forming thin, but dense layers of alumina. A similar phenomenon may occur in voids leading to the presence of alumina on the top wall of the void.

For the case of the irregularly shaped splats, no substrate melting occurs. The molten NiCr particles flatten in a splat, which may be made irregular by the instabilities caused by the gas release from the substrate, which may also cause the formation of some voids at the splat-substrate interface and some oxides within these voids. Upon solidification curling up of the splat was also observed similarly as described before.

3.1.5 Effects of the Mg Content in the Substrate Al Alloy. As it can be observed in the values presented in Table 1, no significant difference was found between the splats formed on the Al 5052 substrates, which contain Mg as a major alloying addition, and Al 1005 substrate, without Mg. Furthermore, the various FIB and TEM cross sections did not show any noticeable difference in structure either. Mg is expected to form a very thin layer of MgO on the surface of the substrate upon heat treatment of the substrate (Ref 28, 30), and, indeed, this was observed on several cross sections (see results presented in a previous study (Ref 28) or such as on Fig. 12 (4) and Fig. 13 (5), as described in a latter section). However, the influence of such layer on splat morphology and formation appears to be negligible, i.e., the surface chemistry difference induced by an Mg addition is not having any noticeable effect.

3.1.6 Effects of Heat Treatment Before Spraying. As discussed in a earlier study (Ref 28), the thermal treatment applied to the aluminum substrate is expected to increase the oxide layer thickness, which is already present on the aluminum substrate as a mixture of oxide (γ-Al_2O_3), oxy-hydroxide and chemisorbed water with a thickness of 2-4 nm, up to ~7 nm. Also, this treatment will partially dehydrate the oxides, resulting in a higher concentration of γ-Al_2O_3, and oxidize the Mg contained in the Al5052 into MgO, as described above.

From analysis of Table 2, it can be concluded that this heat treatment had negligible effects on the various proportions of each type of splat. The partial dehydration from the heat treatment of the oxides layers on the substrate surface, as suggested earlier, could result in less water released from the substrate upon splashing, but this was not observed here, rather no irregular splats with a ring of splashed fingers, hypothetically caused by a significant gas release from the substrate, were found on the thermally treated substrates.

It could also have been expected that the thicker oxide layers increase the thermal contact resistance between substrate and splat, and/or increase the wetting of NiCr, as this was observed when spraying NiCr onto steel substrates (Ref 8, 29). Here, a slight increase in the average diameter of the RSF splats and the irregularly shaped splats, after the thermal treatment, was noted, suggesting that an improvement of the wetting of NiCr may have occurred. However, a decrease for the diameter of the circular splats can also be observed. A possible explanation may be that, as such small splats formed from NiCr fragments splashed away from primary feedstock powder particles upon impact, the impact splashing process becomes modified by the increased roughness, with the rebounding of smaller fragments. Finally, no significant reduction in the degree of substrate melting, which was observed for steel substrates sprayed under similar conditions (Ref 29), could be noted, excluding the possibility of a significant change in the thermal contact resistance between splat and substrate.

3.2 Description of the Splats Found on the Specimen Heated During Spraying

Figure 9 displays SEM images of the different splat morphologies that were found on Al5052_PH:

– The large majority of the splats (62%) found exhibited the morphology shown in Fig. 9(a): a relatively irregular

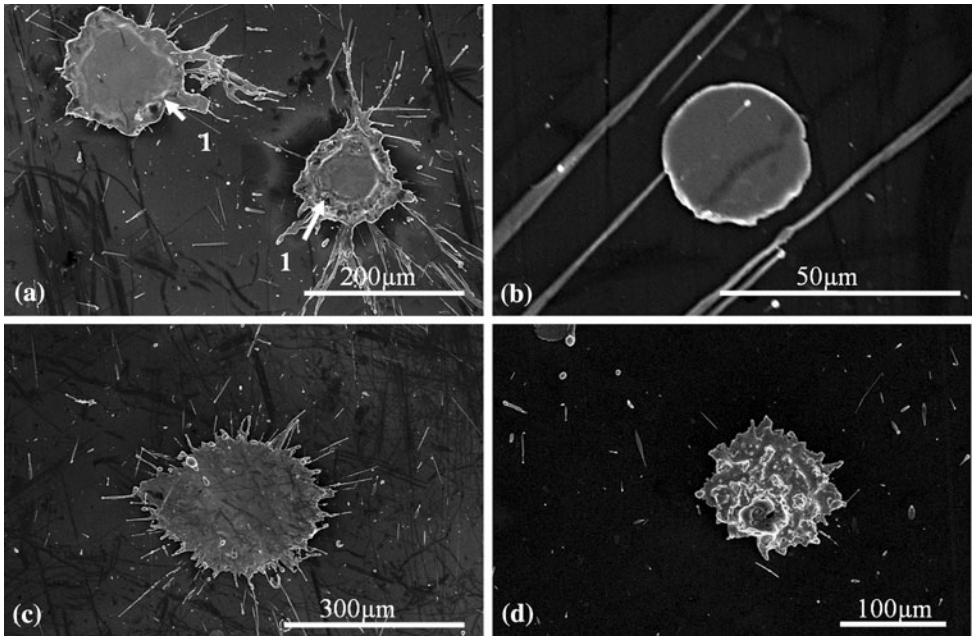

Fig. 9 SEM images of the different types of splats found on Al5052_PH

rim, with a few splashed fingers, but essentially disc-shaped, and outer surface displaying a raised pattern (marked 1). The average diameter D_m was evaluated to be $D_m = [124 \pm 55]$ μm. These splats will be denoted "almost disc-shaped splats."

- Some much smaller splats (24%, $D_m = [30 \pm 10]$ μm) were also found, with usually a very circular shape (see Fig. 9b).These splats will be denoted "small circular splats."
- Splat with a very irregular rim, and a smooth top surface, as shown Fig. 9(c), were also found (11%, $D_m = [196 \pm 46]$ μm). They will be denoted "irregularly shaped splats."
- Finally, very few splats were observed displaying a granular morphology, as if they formed from partially molten NiCr particle (see Fig. 9d, 3%, $D_m = [157 \pm 91]$ μm). They will be denoted "partially melted splats."

3.2.1 Microstructure and Formation Process of the Almost Disc-Shaped Splats. Figure 10 displays a FIB cross section made across such a splat. It can be seen that toward its center, the splat is relatively thin (<1 μm) and flat, with a fine and columnar grain structure. However, toward the splat periphery, the structure is more complex. Mixing of the Al substrate and the NiCr splat has occurred, causing the lift-up of the splat and consequently the raised pattern observed on the SEM image. This shows that localized melting of the substrate has occurred to a significant degree. On the TEM cross section shown in Fig. 11, prepared in a similar location on an almost disc-shaped splat, mixing between splat and substrate can also be observed. On the bright field image (Fig. 11a) and on the EDS elemental maps (Fig. 11b, c), it can be observed how the splat-substrate interface is irregularly shaped and indistinct (1). Some Al is present even on the outer surface of the splat (2). The linescan L1 (see Fig. 11d) made across the interface confirmed the mixing between these phases (3). However, the equilibrium solubility of Ni in Al is negligible and the solubility of Al in Ni is also very limited (<6 wt.%) (Ref 43). Thus, interdiffusion is very less likely compared, for example, to the case of NiCr on stainless steel (Ref 40). On the higher magnification bright field image of the interface (Fig. 11e), a distinct microstructure can be observed, comprising nano-sized grains (4) that become needle-like and normal to the interface on the substrate side (5). Consequently, it is possible that both molten phases, NiCr and Al, intermixed and solidified into a non-equilibrium metastable phase made of a mixture of NiCr and Al nano-sized grains. However, the amorphous layer observed for the splats on the substrate sprayed at room temperature is absent here, probably because solidification for Al5052_PH was slower due to the heating of the substrate.

Also, compared to the previous specimens, the number of splashed fingers is fewer. Heating during spraying above the transition temperature has been known to significantly reduce splashing by preventing gas release from the substrate upon splat formation (Ref 5, 6, 12-15). Consequently, those splashed fingers that were observed may not be caused by the instability from the presence of gas, but rather from the instability caused by the melting of the substrate.

Finally, almost no void or oxide was observed here. This means that the mechanics of the flow of the spreading splat, which led to the formation of large splats within the substrate for the specimens sprayed at room temperature,

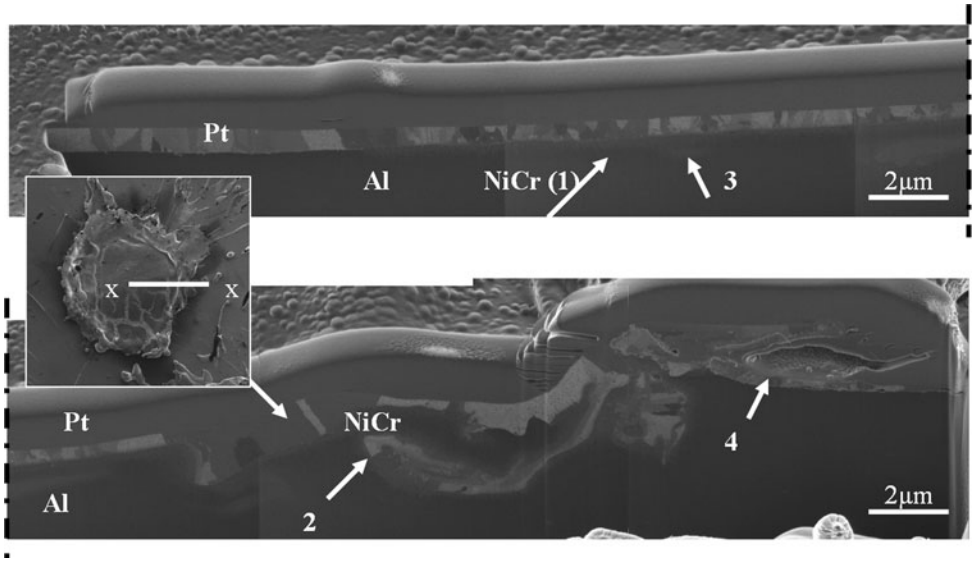

Fig. 10 FIB cross section of an almost disc-shaped splat (see inset picture) found on Al5052_PH

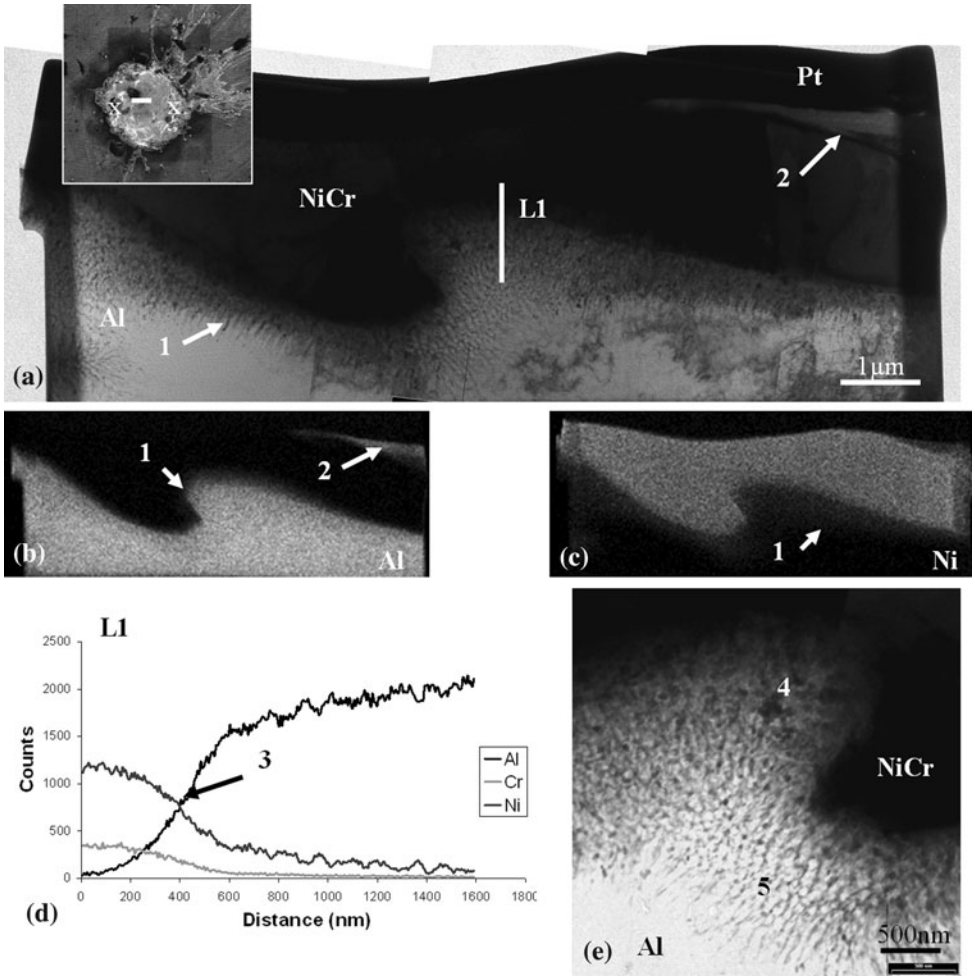

Fig. 11 TEM cross section made across an almost disc-shaped splat (see inset picture) found on Al5052_PH: (a) bright field image, EDS elemental maps for (b) Al, (c) Ni, (d) EDS elemental linescan, and (e) high magnification bright field image of the splat-substrate interface

are modified by the heating of the splat. Another possibility is that the slower solidification rate prevents such voids to form on freezing, but instead, the voids may get filled by flow of the molten material. The absence of smaller voids may also account for the limitation in the amount of gases present at the interface between the substrate and the forming splat.

3.2.2 Microstructure and Formation Process of the Other Types of Splats. While for the almost disc-shaped splats, substrate melting was found to occur, for all the other types of splats formed, no evidence of this phenomenon was observed.

Figure 12 shows a TEM cross section of a small circular splat. It appears very thin (~0.5 μm) (1), with a splat-substrate interface that is both straight and distinct (2). On the EDS elemental maps (Fig. 12c-e), it can be observed that a dense layer of oxide containing Ni and Cr is present around the entire periphery of the splat (3), including at the splat-substrate interface. It was identified by electron diffraction as being spinel $NiCr_2O_4$. As discussed for Fig. 8 (see Sect 3.1.3), the manner in which this oxide forms at the splat-substrate interface is not clear. The shape of the spinel layers, fitting closely the splat, and the formation process of such splat, made from splashed NiCr, make the hypothesis of in-flight oxidation improbable. Since the substrate is heated during this time of formation, oxide may have formed after the splat formation. Such a hypothesis still leaves open the question of the origin of the oxygen for the oxide present under the splat. It is possible that this phase may have arisen from gases released either from the substrate or from the cooling splat (Ref 34). It should be noted that not all small circular splats may present such thick and extended oxide layers, or in some cases maybe Cr_2O_3 rather than spinel. Also, for the splats formed on the 5052 substrates formation of MgO as a thin layer on top of the substrate (4), as discussed earlier, can be observed. See, for example, the Mg EDS elemental map (Fig. 12f).

Moreover, a splat of such dimension (diameter of 30 μm and thickness of 0.5 μm) has a volume which corresponds to a spherical particle of 4.5 μm in diameter. This is thus too small to directly originate from the feedstock powder, especially as there is a relatively large number of small circular splats. As a result, such a splat more probably originates from NiCr fragment splashed away upon impact of a primary NiCr particle, also called ''impact splashing'' (Ref 20, 41).

Figure 13 presents a TEM cross section prepared across the center of an irregularly shaped splat. It can be seen that the splat is quite thick (~4-5 μm) (1) and that the splat-substrate interface is straight and distinct (2). On the EDS elemental maps (Fig. 13d-f) and also on the linescan L1 (Fig. 13g), thin layers of Cr oxide can be observed not only on the top (3) but also the bottom surface of the splat (4), possibly formed because of the heating of the substrate, as well as a thin MgO layer on top of the substrate (5).

For both the small circular splats and the irregularly shaped splats, substrate melting has been inhibited, possibly by the limited temperature and momentum in the case of the small circular splats, or for the other splats a poor contact between the NiCr particle and the substrate. Both Al 5052 and 1005 alloys contain Cr; γ-Al_2O_3 is the most likely oxide expected to form upon oxidation of the substrate, but Cr_2O_3 may form as well (Ref 35). Heating of the substrate may then locally cause formation of such oxides on top of the substrate that would hinder the contact with the NiCr particle and, thus, substrate melting, in the case of the irregularly shaped splats.

Finally, in Fig. 14 is displayed a FIB cross section made across the rim of a partially melted splat. The coarse (2-5 μm) and irregular grain structure (1) is a sign of slow solidification, while some other FIB cross sections showed the presence of zones with still very large (2-7 μm), but equiaxed grains, originating from the initial feedstock powder particles which were found to exhibit such a grain

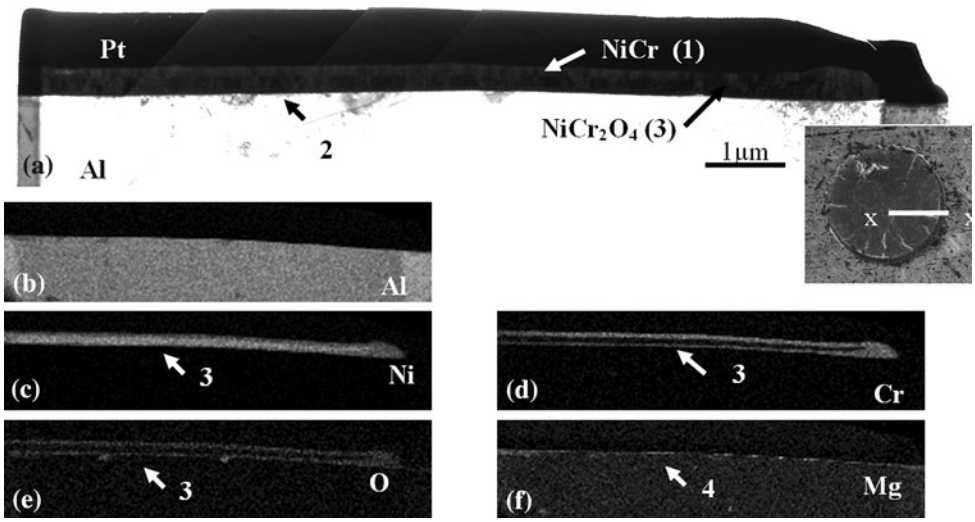

Fig. 12 TEM cross section made across small circular splat (see inset picture) found on Al5052_PH: (a) bright field image, EDS elemental maps for (b) Al, (c) Ni, (d) Cr, (e) O, (f) Mg

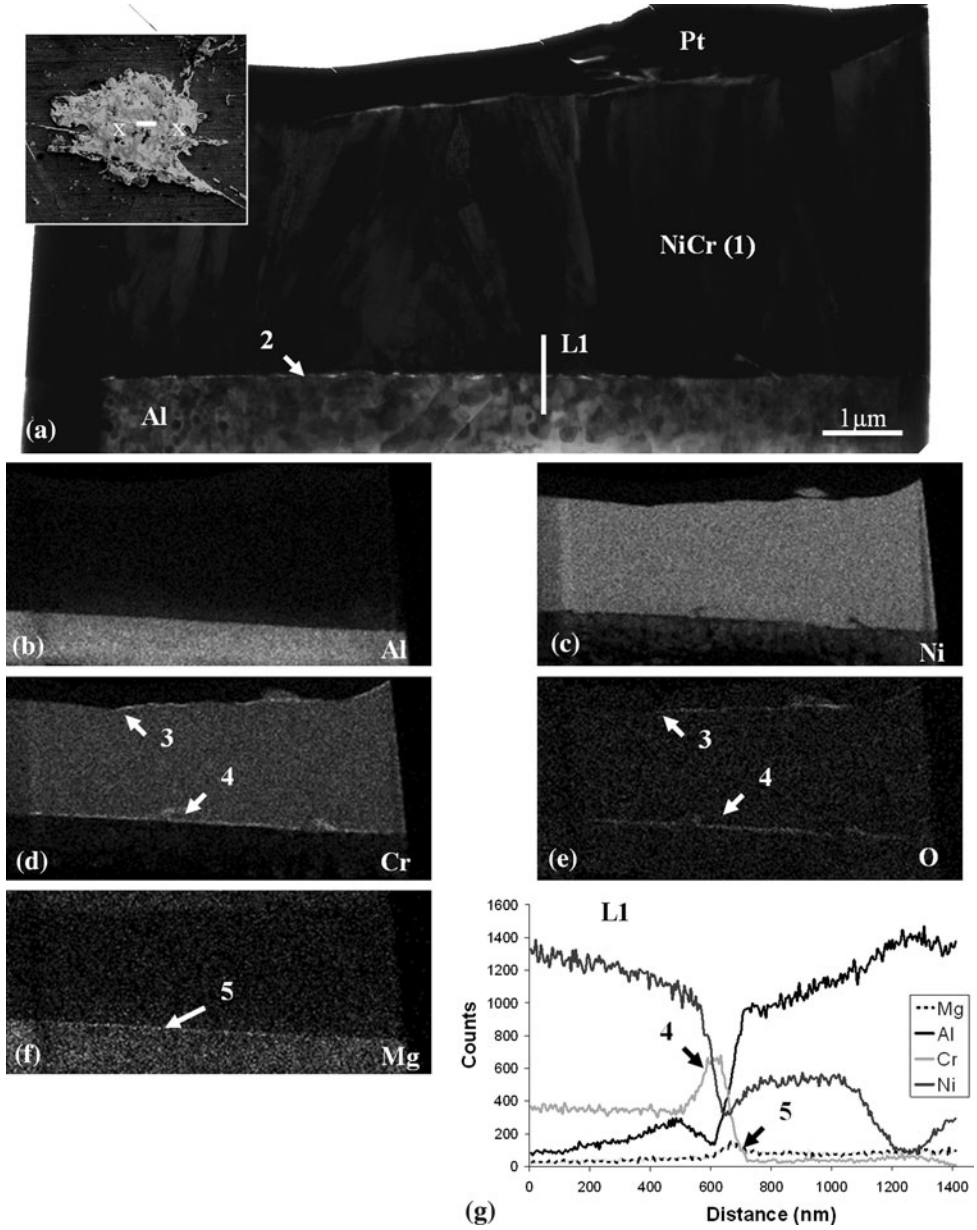

Fig. 13 TEM cross section made across an irregularly shaped splat (see inset picture) found on Al5052_PH: (a) bright field image, EDS elemental maps for (b) Al, (c) Ni, (d) Cr, (e) O, (f) Mg, (g) EDS elemental linescan

structure (Ref 44). Such splats are, as a result, possibly made of a mixture of non-melted fragments and melted zones, solidifying slowly, possibly due to the thickness of such splats (5-10 μm) and the contact with the substrate that may not be uniform, as it can be seen on Fig. 14 as well (2).

3.2.3 Summary of the Splat Formation Process and the Effects of Heating during Spraying. Upon impact of the fully melted NiCr particle, vertical splashing occurs causing the formation of the small circular splats, in the same way as the other Al substrates. Then, due to the heating of the substrate above the transition temperature, desorption of asdorbates/condensates is likely to be very limited, upon impact and spreading of the sprayed particle. Good contact with the substrate is achieved, leading to localized melting of the latter to possibly a slightly greater extent compared to the specimens sprayed at room temperature (due to the better contact and the heat provided by the heating treatment). No, or very limited, splashing of the splat occurs, nor void formation either. However, the molten substrate does get jetted within the flowing NiCr, forming a disordered structure observed at the splat-substrate interface toward the splat periphery, and the raised pattern observed on the top surface of the splat. Solidification of the splat and the molten substrate occurs in the same way for the RSF splats, except that the heating

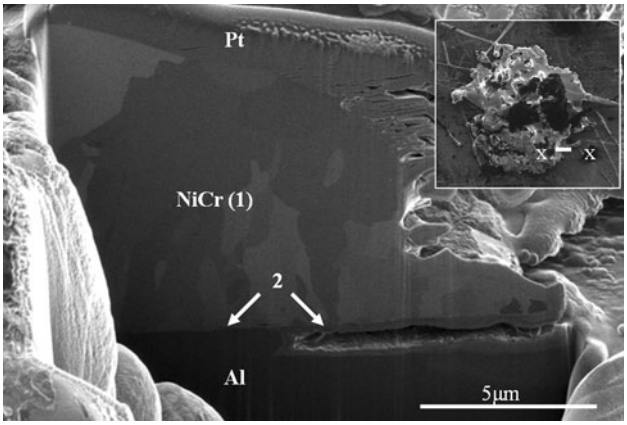

Fig. 14 FIB cross section made across the rim of a partially melted splat (see inset picture) found on Al5052_PH

of the substrate here reduces the solidification rate so that no metallic glass phase is observed.

For the irregularly shaped splats, their formation process is expected to be very similar to the one of the irregularly shaped splats found on the non-heated specimens.

A few partially melted splats were found on the heated specimen. They have formed from sprayed NiCr particles that were only partially molten upon impact. Their lower temperature and the presence of non-melted fragments limited the possibility of substrate melting. Furthermore, such partially molten particle must have also been sprayed onto the non-heated substrate, but presumably must have not adhered to the substrate in this instance. Heating of the substrate must then improve the adhesion of the NiCr particles, leading to the presence of such partially melted particles on the Al5052_PH substrate.

Heating of the substrate may reduce splashing by two ways: reduction or elimination of gas release from the substrate and delaying splat solidification. The almost complete absence of voids also shows the reduction of desorption of gas species from the substrate. In conclusion, heating the substrate during spraying may be beneficial as it significantly reduces splashing along with oxide and voids formation, but also increases the overall adhesion: firstly substrate melting occurs to a greater and deeper extent, without the occurrence of the formation of a potentially brittle phase such as a glassy layer, leading to a stronger metallurgical bonding, and secondly the limitation of voids and splashing means limitation of regions of poor adhesion. Consequently, properties of the complete coatings, such as density, strength, adhesion, etc. will be improved.

4. Conclusion

In order to summarize, the observation of NiCr splats, sprayed on Al substrates, by electron microscopy, led to the following conclusions:

– On the substrates sprayed at room temperature, substrate melting, to a depth up to a few microns, and mixing with melted NiCr was observed for splats with a ring of splashed fingers, but not for the one without splashed fingers. A range of non-equilibrium phases, together with significant concentrations of oxides and voids, was also observed, and where substrate melting occurred, interfacial layers were found, some amorphous and some composed of nano-sized grains, probably formed due to the mixing between NiCr and Al and a rapid solidification. However, the formation mechanisms of some pores and oxide phases are still not fully understood and further study would be required to investigate those.
– Either using an alloy with Mg or heating the substrate before spraying was not found to have a significant effect on splat formation.
– Heating the substrate during spraying was found to result in reduced splashing and potentially slower solidification, leading to the absence of interfacial amorphous layers, and very limited amounts of voids and oxides.

References

1. M. Dorfman, Thermal Spray Basics, *Adv. Mater. Process.*, 2002, **160**(7), p 47-50
2. R.F. Bunshah, *Handbook of Hard Coatings*, Deposition Technologies, Properties and Applications, Norwich, NY, 2001
3. M. Dorfman, Thermal Spray Processes, *Adv. Mater. Process.*, 2002, **160**(8), p 47-49
4. S. Sampath and X. Jiang, Splat Formation and Microstructure Development During Plasma Spraying: Deposition Temperature Effect, *Mater. Sci. Eng.*, 2001, **A304-A306**, p 144-150
5. H. Zhang, X.Y. Wang, L.L. Zheng, and X.Y. Jiang, Studies of Splat Morphology and Rapid Solidification During Thermal Spraying, *Int. J. Heat Mass Transf.*, 2001, **44**, p 4579-4592
6. H. Li, S. Costil, H.-L. Liao, C.-J. Li, M. Planche, and C. Coddet, Effects of Surface Conditions on the Flattening Behavior of Plasma Sprayed Cu Splats, *Surf. Coat. Technol.*, 2006, **200**, p 5435-5446
7. L. Bianchi, A.C. Leger, M. Vardelle, A. Vardelle, and P. Fauchais, Splat Formation and Cooling of Plasma-Sprayed Zirconia, *Thin Solid Films*, 1997, **305**, p 35-47
8. J. Cedelle, M. Vardelle, and P. Fauchais, Influence of Stainless Steel Substrate Preheating on Surface Topography and on Millimeter- and Micrometer-Sized Splat Formation, *Surf. Coat. Technol.*, 2006, **201**, p 1373-1382
9. T. Chraska and A.H. King, Effect of Different Substrate Conditions Upon Interface with Plasma Sprayed Zirconie—A TEM Study, *Surf. Coat. Technol.*, 2002, **157**, p 238-246
10. Z.G. Feng, M. Domaszewski, G. Montavon, and C. Coddet, Finite Element Analysis of Effect of Substrate Surface Roughness on Liquid Droplet Impact and Flattening Process, *J. Therm. Spray Technol.*, 2002, **11**(1), p 62-68
11. A.A. Syed, A. Denoirjean, B. Hannoyer, P. Fauchais, P. Denoirjean, A.A. Khan, and J.C. Labbe, Influence of Surbstrate Surface Conditions on the Plasma Sprayed Ceramic and Metallic Particles Flattening, *Surf. Coat. Technol.*, 2005, **200**, p 2317-2331
12. M. Fukumoto, M. Shiiba, H. Kaji, and T. Yasui, Three-Dimensional Transition Map of Flattening Behavior in the Thermal Spray Process, *Pure Appl. Chem.*, 2005, **77**(2), p 429-442
13. C.-L. Li and J.-L. Li, Evaporated-Gas-Induced Splashing Model for Splat Formation During Plasma Spraying, *Surf. Coat. Technol.*, 2004, **184**, p 13-23
14. M. Fukumoto, E. Nishioka, and T. Matsubara, Flattening Solidification Behavior of a Metal Droplet on a Flat Substrate Surface

Held at Various Temperatures, *Surf. Coat. Technol.*, 1999, **120-121**, p 131-137
15. A. McDonald, C. Moreau, and S. Chandra, Thermal Contact Resistance Between Plasma-Sprayed Particles and Flat Surfaces, *Int. J. Heat Mass Transf.*, 2007, **50**, p 1737-1749
16. X.Y. Jiang, Y. Wan, H. Herman, and S. Sampath, Role of Condensate and Adsorbates on Substrate Surface on Fragmentation of Impinging Molten Droplets During Thermal Spray, *Thin Solid Films*, 2001, **385**, p 132-141
17. M. Fukumoto and Y. Huang, Flattening Mechanism in Thermal Sprayed Nickel Particle Impinging on Flat Substrate Surface, *J. Therm. Spray Technol.*, 1999, **8**(3), p 427-432
18. M. Pasandideh-Fard, V. Pershin, S. Chandra, and J. Mostaghimi, Splat Shapes in a Thermal Spray Coating Process: Simulations and Experiments, *J. Therm. Spray Technol.*, 2002, **11**(2), p 206-217
19. V. Pershin, M. Lufitha, S. Chandra, and J. Mostaghimi, Effect of Substrate Temperature on Adhesion Strength of Plasma-Sprayed Nickel Coatings, *J. Therm. Spray Technol.*, 2003, **12**(3), p 370-376
20. J. Cedelle, M. Vardelle, B. Pateyron, and P. Fauchais, Investigation of Plasma Sprayed Coatings Formation by Visualization of Droplet Impact and Splashing on a Smooth Substrate, *Trans. Plasm. Sci.*, 2005, **33**(2), p 414-415
21. R. Dhiman, A.G. McDonald, and S. Chandra, Predicting Splat Morphology in a Thermal Spray Process, *Surf. Coat. Technol.*, 2007, **201**, p 7789-7801
22. R. Ghafouri-Azar, S. Shakeri, S. Chandra, and J. Mostaghimi, Interactions Between Molten Metal Droplets Impinging on a Solid Surface, *Int. J. Heat Mass Transf.*, 2003, **46**, p 1395-1407
23. S. Goutier, M. Vardelle, J.C. Labbe, and P. Fauchais, Alumina Splat Investigation: Visualization of Impact and Splat/Substrate Interface for Millimetre Sized Drops, *J. Therm. Spray Technol.*, 2010, **19**(1-2), p 49-55
24. J. Mostaghimi and S. Chandra, Splat Formation in Plasma-Spray Coating Process, *Pure Appl. Chem.*, 2002, **74**(3), p 441-445
25. M. Pasandideh-Fard, S. Chandra, and J. Mostaghimi, A Three-Dimensional Model of Droplet Impact and Solidification, *Int. J. Heat Mass Transf.*, 2002, **45**, p 2229-2242
26. S. Kitahara and A. Hasui, A Study of the Bonding Mechanism of Sprayed Coatings, *J. Vac. Sci. Technol.*, 1974, **11**(4), p 747-753
27. L. Li, X.Y. Wang, G. Wei, A. Vaidya, H. Zhang, and S. Sampath, Substrate Melting During Thermal Splat Quenching, *Thin Solid Films*, 2004, **468**, p 113-119
28. S. Brossard, A.T.T. Tran, P.R. Munroe, and M.M. Hyland, Study of the Splat Formation for Plasma Sprayed NiCr on an Al5052 Substrate as a Function of Substrate Condition, *Surf. Coat. Technol.*, 2010. doi:10.1016/j.surfcoat.2010.02.013
29. S. Brossard, P.R. Munroe, A.T.T. Tran, and M.M. Hyland, Study of the Effects of Surface Chemistry on Splat Formation for Plasma Sprayed NiCr onto Stainless Steel Substrates, *Surf. Coat. Technol.*, 2009, **204**(9-10), p 1599-1607
30. R.H. Jones, *Environmental Effects on Engineered Materials*, Marcel Dekker, New York, 2001
31. A.T.T. Tran, M.M. Hyland, T. Qiu, B. Withy, and B.J. James, Effect of Surface Chemistry on Splat Formation During Plasma Spraying, *J. Therm. Spray Technol.*, 2008, **17**(5-6), p 637-645
32. P.R. Munroe, The Application of Focused Ion Beam Microscopy in the Material Sciences, *Mater. Character.*, 2009, **60**, p 2-13
33. L.S. Hung, M. Nastasi, J. Gyulai, and J.W. Mayer, Ion-Induced Amorphous and Crystalline Phase Formation in Al/Ni, Al/Pd, and Al/Pt Thin Films, *Appl. Phys. Lett.*, 1983, **42**(8), p 672-674
34. M. Qu and A. Gouldstone, On the Role of Bubbles in Metallic Splat Nanopores and Adhesion, *J. Therm. Spray Technol.*, 2008, **17**(4), p 486-494
35. C.S. Giggins and F.S. Pettit, Oxidation of Ni-Cr-Al Alloys Between 1000 and 1200 °C, *J. Electrochem. Soc.*, 1971, **118**(11), p 1782-1790
36. M. Xue, S. Chandra, and J. Mostaghimi, Investigation of Splat Curling up in Thermal Spray Coatings, *J. Therm. Spray Technol.*, 2006, **15**(4), p 531-536
37. A.T.T. Tran and M.M. Hyland, The Role of Substrate Surface Chemistry on Splat Formation During Plasma Spray Deposition by Experiments and Simulations, *J. Therm. Spray Technol.*, 2010, **19**(1-2), p 11-23
38. J. Stringer, B.A. Wilcox, and R.I. Jaffee, The High-Temperature Oxidation of Nickel-20 wt.% Chromium Alloys Containing Dispersed Oxide Phases, *Oxid. Met.*, 1972, **5**(1), p 11-47
39. N.S. McIntyre, T.C. Chan, and C. Chen, Characterization of Oxide Structures Formed on Nickel-Chromium Alloy During Low Pressure Oxidation at 500-600 °C, *Oxid. Met.*, 1990, **33**(5/6), p 457-479
40. S. Brossard, P.R. Munroe, A.T.T. Tran, and M.M. Hyland, Study of the Microstructure of NiCr Splats Plasma Sprayed on Stainless Steel by TEM, *Surf. Coat. Technol.*, 2009, **204**(9-10), p 1608-1615
41. C. Escure, M. Vardelle, and P. Fauchais, Experimental and Theoretical Study of the Impact of Alumina Droplets on Cold and Hot Substrates, *Plasma Chem. Plasma Process.*, 2003, **23**(2), p 185-221
42. H. Beck and H.-J. Güntherodt, *Glassy Metals*, Springer-Verlag, Berlin, 1983
43. T.B. Massalski, H. Okamoto, P.R. Subramanian, and L. Kacprzak, *Binary Alloy Phase Diagrams*, 2nd ed., ASM International, Materials Park, Ohio, 1990
44. W.J. Trompetter, M. Hyland, P. Munroe, and A. Markwitz, Evidence of Mechanical Interlocking of NiCr Particles Thermally Sprayed onto Al Substrates, *J. Therm. Spray Technol.*, 2005, **14**(4), p 524-529